Spray drying of poorly soluble drugs from aqueous arginine solution

Rami Ojarinta[a, *], Louise Lerminiaux[a, b], Riikka Laitinen[a]

[a] School of Pharmacy, University of Eastern Finland, P.O. Box 1627, 70211 Kuopio, Finland

[b] Laboratory for Pharmaceutical Process Analytical Technology, Department of Pharmaceutical Analysis, Faculty of Pharmaceutical Sciences, Ghent University, Ottergemsesteenweg 460, 9000 Ghent, Belgium

*Corresponding author:

Tel. +358 40 355 3870

E-Mail: rami.ojarinta@uef.fi

ABSTRACT

Co-amorphous drug-amino acid mixtures have shown potential for improving the solid-state stability and dissolution behaviour of amorphous drugs. In previous studies, however these mixtures have been produced mainly with small-scale preparation methods, or with methods that have required the use of organic solvents or other dissolution enhancers. In the present study, co-amorphous ibuprofen-arginine and indomethacin-arginine mixtures were spray dried from water. The mixtures were prepared at two drug-arginine molar ratios (1:1 and 1:2). The properties of the prepared mixtures were investigated with differential scanning calorimetry, X-ray powder diffractometry, Fourier-transform infrared spectroscopy and a 24h, non-sink, dissolution study. All mixtures exhibited a single glass transition temperature (T_g), evidence of the formation of homogenous single-phase systems. Fourier transform infrared spectroscopy revealed strong interactions (mainly salt formation) that account for the positive deviation between measured and estimated T_g values. No crystallization was observed during a 1-year stability study in either 1:1 or 1:2 mixtures, but in the presence of moisture, handling difficulties were encountered. The formation of co-amorphous salts led to improved dissolution characteristics when compared to the corresponding physical mixtures or to pure crystalline drugs.

KEYWORDS: Co-amorphous, amino acid, spray drying, stability, dissolution

ABBREVIATIONS[1]

[1] ARG, arginine; ACN, acetonitrile; DSC, differential scanning calorimetry; FTIR; Fourier-transform infrared spectroscopy; HPLC, high performance liquid chromatography; IBU, ibuprofen; IND, indomethacin; RH, relative humidity; SD, spray dried; TFA, trifluoro acetic acid; Tg, glass transition temperature; Tm, melting temperature; Trc, recrystallization temperature; XRPD, X-ray powder diffractometry

1. INTRODUCTION

If orally administered drugs are to be bioavailable, they have to possess sufficient water solubility. For some drugs (Biopharmaceutical classification system; Class II), the dissolution may even be the rate limiting step in drug absorption (Baghel et al. 2016). However, since the advent of combinatorial chemistry and high throughput screening techniques, the water solubility of new drug candidates has decreased drastically (Lipinski et al. 2001).

Utilizing the amorphous form of a drug is one of the numerous formulation methods intended to improve its dissolution properties (Laitinen et al. 2013). The increase in apparent solubility and hence bioavailability, is due to the higher internal energy in the amorphous form compared to the crystalline counterpart. On the other hand, this property may cause the amorphous drug to recrystallize during processing, storage, or dissolution. Nevertheless, it is now well established that with a proper selection of a polymer, the polymeric amorphous solid dispersion approach may improve the solid-state stability of the amorphous form as well as increase the stability of the supersaturated state in a solution (Baghel et al. 2016; He and Ho 2015). Despite intensive research, however, only a few amorphous solid dispersion based formulations have reached the global market (He and Ho 2015). There are several challenges associated with these polymers e.g. the poor miscibility of some drugs with polymers, the hygroscopicity of polymers, incompatibility issues, and other poor formulation characteristics, such as poor flowability or compressibility (Löbmann et al. 2011).

In an attempt to avoid the use of polymers, another subclass of solid dispersions, namely co-amorphous formulations, has been introduced (Dengale et al. 2016; Laitinen et al. 2013). In co-amorphous formulations, low molecular weight compounds are used instead of polymers to form an amorphous homogenous single-phase mixture (Dengale et al. 2016). In order to prepare co-amorphous systems, both pharmaceutically active substances and inactive excipients have been used, and both approaches have successfully stabilized the amorphous form and enhanced the dissolution

properties of the studied drugs (Allesø et al. 2009; Jensen et al. 2014; Löbmann et al. 2011; Löbmann et al. 2013a).

It is known that the preparation method may affect certain properties of the amorphous drugs, such as their glass transition temperature (T_g), dissolution, and stability (Agrawal et al. 2013; Sakurai et al. 2012; Zhang et al. 2009). Preparation techniques of amorphous formulations can be roughly divided into fusion or melting techniques (e.g. melt quenching, hot melt extrusion), solvent techniques (e.g. solvent casting, freeze drying, spray drying), and techniques that involve mechanical activation (e.g. cryogenic grinding) (Baghel et al. 2016; Meng et al. 2015; Vasconcelos et al. 2016). A wide range of these techniques has been applied to manufacture the polymeric amorphous solid dispersions, but due to the several advantages, such as scalability from laboratory to industrial scale and option for continuous manufacturing, the hot melt extrusion and spray drying techniques have become the most popular techniques both in laboratory and especially on the industrial scale (Van Den Mooter 2012; Vasconcelos et al. 2016; Vo et al. 2013). Nonetheless, the majority of co-amorphous formulations have been prepared by less scalable and less efficient methods, such as melt quenching and ball milling (Chavan et al. 2016; Meng et al. 2015; Vasconcelos et al. 2016). During recent years, however, also the use of spray drying from organic solvents has been shown to be applicable for co-amorphous formulations (Beyer et al. 2016b; Craye et al. 2015; Jensen et al. 2016a).

In spray drying, a solution containing the solvent and the components of the co-amorphous mixture is sprayed into a hot air stream, with the rapid evaporation of the solvent, and the formation of homogenous amorphous solid particles (Vasconcelos et al. 2016). Additional advantages of spray drying against melting methods include the relatively low processing temperatures and beneficial particle morphology (Baghel et al. 2016). The challenge in the preparation of co-amorphous formulations via spray drying is to find a common solvent suitable for all the components, especially when combining a poorly water-soluble drug with a readily-soluble co-former. Since it is important to avoid the use of toxic and environmentally hazardous organic solvents, excipients, such as

surfactants may be needed to enhance the dissolution of the drug, and subsequently to enable the spray drying (Craye et al. 2015). However, some tolerability issues may also be associated with the surfactants (Baghel et al. 2016). Thus, it would be preferable to find co-formers that alone would enhance the dissolution of the drug adequately to enable the spray drying from aqueous solutions containing only the co-former and the drug.

In the present study, co-amorphous mixtures of arginine (ARG) with ibuprofen (IBU) and indomethacin (IND) were prepared by spray drying. Unlike in the previous studies investigating spray drying co-amorphous formulations, only pure water was used as a solvent in order to avoid the challenges associated with additional excipients (Baghel et al. 2016; Beyer et al. 2016b; Craye et al. 2015; Jensen et al. 2016a). We also prepared the co-amorphous mixtures in a molar ratio of 1:2 in addition to the commonly utilized molar ratio of 1:1, since Jensen et al. (2016b) observed that with co-amorphous IND-ARG mixtures, the molar ratio of 1:1 may not possess the highest T_g values. The properties of these mixtures were then investigated with X-ray powder diffraction (XRPD), Fourier-transform infra-red spectroscopy (FTIR), and differential scanning calorimetry (DSC) to verify the changes in their solid-state, and to examine their physical stability. Additionally, the dissolution properties of the mixtures were studied in 24h dissolution tests.

2. MATERIALS AND METHODS

2.1 Materials

IND was purchased from Hangzhou Dayanchem (Hangzhou, China), ARG from Sigma-Aldrich (Riedel-de Haan, Germany), and IBU was kindly donated by Orion Pharma (Espoo, Finland) (see Figure 1 for chemical structures). Sodium chloride (NaCl; J.T. Baker, Deventer, Holland), hydrochloric acid (HCl, 37 %; Riedel-de-Haën, Seelze, Germany), potassium dihydrogen phosphate (KH_2PO_4; Merck, Darmstadt, Germany), sodium hydroxide (NaOH; VWR Chemicals, Leuven, Belgium), and glacial acetic acid (Riedel de Haën, Germany) were used to prepare the buffer solutions

115 (pH 1.2, 5.0 and 7.2). Phosphorus pentoxide (P_2O_5) was used to maintain 0% and sodium bromide
116 (NaBr) to ensure 60% relative humidity (RH) conditions during storage.

117 Purified (class II; Elix 5, Millipore S.A.S., Molsheim, France) and ultrapurified (class I; Elga Purelab
118 Ultra, Elga LabWater, UK) water were used throughout the study. If not specified, class II water was
119 used. Acetonitrile (ACN; HiPerSolv for HPLC, VWR Chemicals, Leuven, Belgium) and trifluoro
120 acetic acid (TFA, 55.5%; HPLC grade, Alfa Aesar, Karlsruhe, Germany) were used as components
121 of the high performance liquid chromatography (HPLC) mobile phase.

122 **2.2 Methods**

123 **2.2.1 Phase solubility test**

124 To explore the effect of the ARG concentration on the solubilities of the model drugs, we added an
125 excess of both drugs to 20 ml of 1%, 5% and 10% (m/V) ARG-water solution. The study was
126 performed in triplicate in 50 ml Erlenmeyer flasks containing a magnetic stirrer bar (ambient
127 conditions). After 3 days of stirring, a 5 ml sample from each flask was filtered through 0.22 µm
128 membrane filter (Syringe Filter 30 mm Dia, PES 0.22 µm Membrane, Sterile, Porvair Sciences), and
129 the filtrate was diluted with an adequate amount of 70/30 (V/V) ACN/class I water-mixture to reach
130 concentrations between 1 and 100 µg/ml.

131 **2.2.2 High Performance Liquid Chromatography (HPLC)**

132 The drug concentrations were measured in an HPLC that consisted of Gilson 321 pump, Gilson UV-
133 vis 151 detector (both from Gilson Inc., Middleton, WI, USA), Gilson 234 auto injector (Gilson,
134 Roissy-en-France, France), and a reversed phase column (Phenomenex Gemini NX 5u C18 110A,
135 250x4, 60 mm, sr. nr. 590531-19, USA) with a pre-column. The mobile phase flow rate was set at
136 1.2 ml/min and the detection wavelengths were 221 nm for IBU and 225 nm for IND. The mobile
137 phase consisted of 70% of ACN and 30% of class I water, which were acidified by addition of 0.1%
138 of TFA.

We prepared a 100 µg/ml standard solution from both drugs by weighing 10 mg of drug and dissolving it into 100 ml of 70/30 ACN/class I water-mixture. Other standard solutions (1, 5, 12.5, 25, 50 µg/ml) were prepared by diluting the 100 µg/ml solution. Each standard solution was analysed by HPLC to obtain standard lines that were found to be linear ($R^2 > 0.997$) in the examined concentration range.

2.2.3 Spray drying

Spray drying was conducted with a Büchi Mini Spray Dryer B-191 (Büchi Labortechnik AG, Flawil, Switzerland). The correct amount of crystalline drug was dissolved into 5 % (m/V) ARG-class 1 water-solution to achieve drug-ARG-molar ratios of 1:1 or 1:2. When the drugs were completely dissolved (no solid material left) the solutions were spray dried under following conditions: inlet temperature 160 °C, outlet temperature 83 ± 6 °C, air flow rate 600 l/h, and pump rate 5.3 ± 0.2 ml/min. The correct molar ratios of the prepared powders were confirmed by completely dissolving an amount of mixtures corresponding to 20 mg of the drugs and measuring the total amount of dissolved drug by HPLC (see supplementary material; Table S1).

2.2.4 Cryomilling

Crystalline IND was converted into an amorphous form in an oscillatory ball mill (Mixer Mill MM400, Retsch GmbH & Co., Haan, Germany). A total of 500 mg of crystalline drug was placed in a 25 ml milling chamber with two 12 mm stainless steel balls. The chambers were immersed in liquid nitrogen for two minutes prior to milling and every 10 minutes during the milling. The milling time was 60 min at 30 Hz milling frequency.

2.2.5 Preparation of IBU-ARG salt by slowly evaporating water

To investigate whether a crystalline IBU-ARG salt could be produced by slowly evaporating the solvent, 300 mg of IBU and a corresponding amount of ARG were dissolved in 5 ml of water to produce IBU-ARG solutions of molar ratios of 1:1 and 1:2. Since the components had dissolved, the

solution was placed on a Petri dish, and the water was allowed to evaporate over 3 days in ambient conditions in a fume hood. The resulting solid material was investigated with XRPD and FTIR.

2.2.6 Differential scanning calorimetry (DSC)

Thermal analyses were conducted using Mettler Toledo DSC823^e apparatus (Mettler-Toledo, Schwerzenbach, Switzerland) equipped with an inter-cooler (Mettler-Toledo, METT-FT900 Julabo, Switzerland) and an autosampler (TS080IRO Sample Robot, Mettler-Toledo, Schwerzenbach, Switzerland). Thermograms were obtained under a nitrogen gas flow (50 ml/min). Approximately 5 mg of sample powder was placed into a 40 µl aluminium pan, which was sealed with a pierced lid.

The temperature settings of the DSC runs for different materials can be found from the supplementary material (Table S2). For crystalline drugs, two heating cycles were performed to produce the pure amorphous drug by in situ quench cooling, which enabled the measurement of melting temperature (T_m) of crystalline drug (first cycle) and glass transition temperature (T_g) of amorphous drug (second cycle). Spray dried samples were measured using temperature modulated DSC (TOPEM®, Mettler-Toledo, Schwerzenbach, Switzerland) to eliminate the effect of residual moisture. For crystalline ARG, only one-cycle conventional DSC run was performed, since the production of amorphous ARG via quench cooling has been shown to be impossible (Löbmann et al. 2013a).

Theoretical T_g-values of the co-amorphous mixtures were calculated using Gordon-Taylor equation (Eq. 1):

$$T_g(mix) = \frac{w_1 T_{g1} + K w_2 T_{g2}}{w_1 + K w_2} \quad (1)$$

where T_g(mix) is the theoretical glass transition temperature of the mixture, w_1 and w_2 are the weight fractions and T_{g1} and T_{g2} are the glass transition temperatures of the individual mixture components, and K is a constant, which can by defined by Eq. 2:

$$K = \frac{T_{g1} \times \rho_1}{T_{g2} \times \rho_2} \quad (2)$$

where ρ_1 and ρ_2 are the densities of the two components. The densities of crystalline instead of amorphous components were used as approximation. This approximation has been previously justified by the small difference in powder densities between crystalline and amorphous small-molecular compounds (Löbmann et al. 2011; Löbmann et al. 2013a).

2.2.8 Fourier transform infrared spectroscopy (FTIR)

FTIR-analyses were performed using Thermo Nicolet Nexus 8700 spectrometer (Thermo Electron Corp., Madison, WI, USA) with attenuated total reflectance accessory. Average spectra of 64 scans with the resolution of 4 cm^{-1} were collected over a wave number range of 650-4000 cm^{-1}. The results were analyzed using Thermo Scientific OMNIC software (version 6.0a, Thermo Scientific).

2.2.9 X-ray powder diffraction (XRPD)

Bruker D8 Discover diffractometer (Bruker AXS GmbH, Karlsruhe, Germany) with Cu Kα radiation (λ = 1.54 Å) was applied to perform XRPD-analyses. The scan was performed between 5 and 35° 2θ with scan speed of 0.1 s/step and step size of 0.011°. An acceleration voltage of 40 kV and a current of 40 mA were used. The results were analyzed by DIFFRAC.V3 program (Bruker AXS GmbH).

2.2.10 Stability studies

To investigate the stability of amorphous state in different conditions, the prepared amorphous materials were kept under 4 °C/0% RH, 25 °C/60% RH, and 40 °C/0% RH. 0% RH was obtained by using P_2O_5 and 60 % RH by using a saturated NaBr solution. To observe the changes in the solid state, the materials were repeatedly analyzed with XRPD and FTIR.

2.2.11 Dissolution studies

Dissolution behavior of the materials was investigated with Sotax AT7 smart and Sotax AT6 dissolution testers (Sotax AG, Basel, Switzerland) equipped with paddle stirrers. A total of 20 mg of drug or an amount of drug-ARG mixture corresponding to 20 mg of drug was placed in triplicate in

500 ml of either hydrochloric acid buffer (pH 1.2; SIF Powder Original® How To Use 1.4, 2013), acetate buffer (pH 5.0; SIF Powder Original® How To Use 1.4, 2013) or phosphate buffer (pH 7.2; USP)). The dissolution media was kept at 37 °C, and it was stirred for 24 h at 50 rpm. Samples (5 ml) were taken at 15 min, 30 min, 1h, 1.5h, 2h, 4h, 6h, 8h and 24h and filtered through a 0.22 µm membrane filter (Syringe Filter 30 mm Dia, PES 0.22 µm Membrane, Sterile, Porvair Sciences, Leatherhead, UK). The sample volume was replaced with pure buffer solution. The drug concentration of the samples was analyzed with HPLC.

2.2.12 Statistical analysis

The statistical analyses (single-factor ANOVA with Tukey's post-hoc test, linear regression) were conducted with GraphPad Prism 5.03 (GraphPad Software Inc., La Jolla, USA). The results were considered statistically significant if $p < 0.05$.

3. RESULTS AND DISCUSSION

3.1 Phase solubility test

The equilibrium solubilities of IBU and IND in 1, 5, and 10% (m/V) ARG solutions after 72h solubility test are presented in Table 1. The statistical analysis revealed significant differences in IBU concentrations between 1 and 5% (m/V) ARG solutions, whereas the IND concentrations differed significantly between every ARG solution. The linear regression analysis suggests that there was a nearly linear increase ($R^2 = 0.9522$) in IND concentration as the ARG concentration was elevated. With IBU, the linearity was less obvious ($R^2 = 0.6950$).

The effect of ARG concentration on IND solubility has been studied also by ElShaer et al. (2011). Although their study was conducted with smaller ARG concentrations (0.001-0.1% (m/V)), a linear relationship between ARG and IND concentrations was observed. This linearity was attributed to the total dissociation of IND in ARG solution, which promoted salt formation between these two species. With IBU and ARG, we were unable to find phase solubility diagrams in the published literature, but

231 it has been shown that the IBU-ARG salt dissolved more rapidly when compared to the free acid
232 (Bruzzese and Ferrari 1981; Fini et al. 1985; Stroppolo et al. 1995). Additionally, at low pH values,
233 the salt form seemed to maintain a higher cumulative amount dissolved at least for the first 500
234 minutes when compared to the free acid (Fini et al. 1985).

235 **3.2 Spray drying**

236 Based on the phase solubility test, the 5% (m/V) ARG solution was chosen as the solvent for spray
237 drying co-amorphous drug-ARG mixtures, since it produced drug-ARG solutions of a molar ratio
238 close to 1:1 with both IBU and IND, and the solvent volumes remained relatively small, even with
239 increased batch sizes. Additionally, pure ARG was spray dried from a 5% solution.

240 Spray drying different drug-amino acid mixtures (from organic solutions) has previously resulted in
241 yields of approximately 70% (Jensen et al. 2016a). In our study, the average yields with drug-ARG
242 mixtures varied from 29.2% to 34.4%. The lower yields may be attributed to different process
243 parameters (Lipiäinen et al. (2016)), which were not further optimized, since a satisfactory amount
244 of material was produced to perform the desired analyses. Spray drying of pure ARG resulted in a
245 yield of only 3.5%, which was not unexpected based on the study of Lakio et al. (2015), who failed
246 to spray dry pure ARG due to the hygroscopicity of the product, and the consequent lack of yield.
247 Despite the low yield also in the present study, enough material was produced to gain some insight
248 into the properties of the spray dried ARG.

249 **3.3 Solid-state characterization**

250 3.3.1 X-Ray Powder Diffraction

251 The halo patterns in the X-ray diffractograms (Figure 2) confirmed that all spray dried drug-ARG
252 mixtures as well as cryomilled IND were amorphous. With spray dried ARG, only minor peaks could
253 be observed at 2θ-values of approximately 18.2°, 19.0°, 22.9°, and 27.3°, evidence that the material
254 was mainly amorphous. However, the attempts to cryomill or quench cool pure IBU were

255 unsuccessful in producing amorphous IBU, as shown by the peaks characteristic for crystalline IBU
256 in Figure 2. The instability of the amorphous IBU may be attributed to the very low T_g (Table 2). At
257 ambient conditions, this leads to the rapid molecular movement and the consequent immediate
258 crystallization of IBU (Laitinen et al. 2013).

259 We were unable to find previous attempts to produce amorphous IBU-ARG mixtures, but the
260 preparation of crystalline IBU-ARG salt has been introduced in U.S. patents 4,279,926 and 5,463,117
261 (Bruzzese and Ferrari 1981; Stroppolo et al. 1995). The method in U.S. patent 4,279,926, however,
262 requires the use of an organic solvent (acetone), and apparently the use of the more expensive DL-
263 ARG instead of L-ARG, since two groups have been unable to produce crystalline salt from IBU and
264 L-ARG (Bruzzese and Ferrari 1981; Cristofoletti and Dressman 2017; Lee and Wang 2009). The U.S.
265 patent 5,463,117 describes a preparation method where no organic solvents are required and the salt
266 is produced from L-ARG, but this method seems to contain several energy (and time) consuming
267 phases (Stroppolo et al. 1995). In the present study, we aimed to produce crystalline IBU-ARG salt
268 by slowly evaporating the water; this was thought to allow the IBU and ARG molecules to form an
269 ordered crystal structure. However, as observed with IND-ARG 1:1 mixture prepared in a similar
270 manner (Ojarinta et al. 2017), a halo pattern was observed in the diffractogram (Figure 2) of the dry
271 product indicating the formation of an amorphous salt.

272 In the situation that the amorphous form of the IBU-ARG mixture proves to be stable over a sufficient
273 time period, possesses improved dissolution properties when compared to crystalline IBU, and the
274 end product is in the form of IBU-ARG salt, the spray drying method described in the present study
275 may provide a viable option for the preparation methods in the cited patents. The benefits of this
276 method include the use of water as the sole solvent, the use of L-ARG instead of DL-ARG or D-
277 ARG, and the production of dry powder ready for further processing through a single process step.
278 Additionally, less heat stress is directed to the drug when compared to the method in U.S. patent
279 5,463,117, since no melting of the drug is required.

The co-amorphous IND-ARG 1:1 mixture has been prepared previously by both cryomilling and spray drying, and both preparation methods have been shown to produce stable co-amorphous mixture with enhanced dissolution characteristics (Jensen et al. 2016a; Löbmann et al. 2013a). However, as far as we are aware, this is the first time that co-amorphous IND-ARG has been spray dried from water, which minimizes the risk of residual organic solvents remaining in the final product. Additionally, the production of amorphous ARG has been previously shown possible via freeze drying (Izutsu et al. 2005), but according to the present study, spray drying may also result in at least mainly amorphous ARG. Due to the low yields and some crystalline residues, this method, however requires further adjustment, and may be only suitable for research purposes.

3.3.2 Differential Scanning Calorimetry

The co-amorphous mixtures exhibited a single T_g (Table 2, full thermograms in the supplementary material (Figures S1 and S2)), which is widely used as an indicator for a homogenous single phase system (Jensen et al. 2016a; Löbmann et al. 2013a). The T_g of spray dried IND-ARG 1:1 was rather consistent with the T_gs measured by Jensen et al. (2016a) for both cryomilled and spray dried mixtures (117.5 °C and 114.1 °C, respectively). These values, however, are markedly higher when compared to previous measurements from cryomilled IND-ARG mixtures (62.9 °C (Ojarinta et al. 2017) and 64.1 °C (Löbmann et al. 2013a)). The higher T_g values have been obtained with temperature modulated DSC programs, which suggests that moisture may have interfered with the interpretation of the thermograms from conventional DSC.

The T_gs of all the single components could be obtained from the cryomilled, quench cooled or spray dried samples (Table 2, Figure S3). However, with spray dried ARG, the T_g was only visible with one DSC sample, but the exothermic recrystallization peak (T_{rc} (onset): 105 ± 0.3 °C) was observed in non-reversing and total heat-flow plots of both of the measured samples. With IBU and IND, the T_gs were consistent with the values previously reported, but with ARG, the deviation was more pronounced. This phenomenon may be explained by the hygroscopicity and varying water content of

305 the amorphous ARG (Jensen et al. 2016b). Based on their predictions, Jensen et al. suggested that 55
306 °C would be the most correct T_g for ARG, and that value was selected for Gordon-Taylor calculations
307 also in our study.

308 The Gordon-Taylor equation is a widely used tool for predicting the T_gs of multicomponent systems
309 (Baird and Taylor 2012). The deviations from the predicted values have been considered as signals
310 of improper mixing or interactions between molecules, since the equation assumes the ideal volume
311 additivity of the components and the lack of interactions between them. In the present study, positive
312 deviations from predicted values were observed with both drug-ARG combinations at both molar
313 ratios (Table 2). In fact, the T_gs of the binary mixtures were higher than the T_g of either single
314 component with both IBU-ARG and IND-ARG mixtures regardless of the molar ratio. This
315 observation suggests strong interactions between the components of the co-amorphous mixtures.

316 With co-amorphous IND-ARG 1:1 as well as naproxen-ARG mixtures, the formation of amorphous
317 salt has been demonstrated previously (Jensen et al. 2014; Löbmann et al. 2013c). Due to the presence
318 of a carboxylic acid group in the IBU structure, and the existence of crystalline IBU-ARG salt
319 mentioned in section 3.3.1, the salt formation probably plays a role also in co-amorphous IBU-ARG
320 1:1 mixture. However, with IBU-ARG, the T_g of the 1:2 mixture was approximately identical or even
321 slightly higher when compared to the 1:1 mixture, even though the salt is formed between one drug
322 molecule and one ARG molecule. This phenomenon was also observed by Jensen et al. (2016b), who
323 investigated the co-amorphous IND-ARG mixtures of different molar ratios, and observed that the
324 highest T_g appeared at the molar ratio of 40% drug and 60% ARG.

325 3.3.3 Fourier-Transform Infrared Spectroscopy

326 The FTIR measurements were conducted to investigate the interactions between the drug and ARG,
327 which were assumed based on the DSC measurements. The wave number region from 1000 to 1800
328 cm^{-1} was evaluated, since the major differences in the spectra were observed in that region. The

329 spectra of the pure crystalline substances (Figure S4) were in good accordance with the previous
330 measurements (Kyerematenga et al. 2014; Löbmann et al. 2013b; Löbmann et al. 2013c). In addition,
331 the differences in the spectrum of amorphous IND when compared to the spectrum of γIND
332 corresponded well with previous findings (Löbmann et al. 2013b). Unfortunately, we were unable to
333 measure the spectrum of amorphous IBU, but according to Kyerematenga et al. (2014), only general
334 band broadening and a slight shift of the aromatic C=C stretching band (1508 cm^{-1} in our crystalline
335 sample) may occur in the spectrum of amorphous IBU.

336 In the spectrum of spray dried ARG (Figure S4), the peaks were broader and less intense when
337 compared to crystalline ARG, which has been observed previously with amorphous material
338 (Löbmann et al. 2013b). The band shifts between the spectra of crystalline and amorphous ARG
339 included the shift from 1675 cm^{-1} (COO^- and guanidyl group stretching (Löbmann et al. 2013c)) to a
340 shoulder at 1668 cm^{-1}, from 1613 cm^{-1} (guanidyl group stretching (Löbmann et al. 2013c)) to 1632
341 cm^{-1}, from 1552 cm^{-1} (CN stretch (Löbmann et al. 2013c)) to 1540 cm^{-1}, and from 1420 cm^{-1} (COO^-
342 stretching (Löbmann et al. 2013c)) to 1405 cm^{-1}. These findings were highly inconsistent with the
343 spectrum of freeze dried ARG (Jensen et al. 2016a), which to some extent could be attributed to
344 different molecular arrangements caused by different preparation methods. However, the reliability
345 of the spectrum of the freeze dried ARG seemed questionable due to the total disappearance of the
346 intense peaks of crystalline ARG between 1500 cm^{-1} and 1700 cm^{-1}.

347 The FTIR spectra of the co-amorphous IBU-ARG and IND-ARG mixtures (Figure 3) are presented
348 together with the calculated addition spectra of the corresponding drug and ARG. With IND-ARG,
349 the addition spectrum was formed using the spectra of amorphous components, but with IBU-ARG
350 the spectrum of crystalline IBU was used in the formation of the addition spectrum. This was
351 considered justified, however, due to the minor differences between the spectra of crystalline and
352 amorphous IBU (Kyerematenga et al. 2014).

353 The most significant change in the spectra of the co-amorphous mixtures of both molar ratios when
354 compared to the calculated addition spectra was the total disappearance of the carboxylic acid bands
355 of both drugs (1699 cm^{-1} in IBU-ARG addition spectrum and 1705 cm^{-1} and 1735 cm^{-1} in IND-ARG
356 addition spectrum). In addition, a peak shift from 1540 cm^{-1} (CN stretch) to a higher wave number
357 was observed in the spectra of co-amorphous IND-ARG 1:1 (1552 cm^{-1}) and 1:2 (1547 cm^{-1})
358 mixtures. Additionally, the ARG COO^- stretching band at 1401 cm^{-1} in the IND-ARG addition
359 spectrum, and the combination of ARG COO^- stretching and IBU CO-H bending bands at 1418 cm^{-1}
360 in the IBU-ARG addition spectrum had shifted to a lower wave number (1389-1395 cm^{-1}). The
361 spectra of IBU-ARG mixtures prepared by slow evaporation resembled the spectra of the co-
362 amorphous mixtures. This similarity is evidence of equivalent interactions between molecules
363 regardless of the preparation method, which was also observed with IND-ARG mixture in our
364 previous study (Ojarinta et al. 2017).

365 Previously, the absence of the carboxylic acid bands combined with changes in the ARG CN
366 stretching environment have been assigned to salt formation between IND and ARG (Löbmann et al.
367 2013c). In the present study, both of these features existed in the spectra of co-amorphous IND-ARG
368 mixtures, but only the disappearance of the carbonyl peak could be observed in the spectra of co-
369 amorphous IBU-ARG mixtures. Nevertheless, considering the chemical nature of IBU and ARG as
370 well as the clear change caused by co-amorphization in the carboxylic acid region of the FTIR
371 spectrum of IBU, it seems that salt formation probably accounts for the positive deviation in the
372 measured T_gs of the co-amorphous IBU-ARG mixtures as well. The changes in ARG COO^- stretching
373 band and IBU CO-H bending band may indicate further interactions, such as hydrogen bonding,
374 between the drugs and ARG. Additionally, ARG has been previously shown to interact with aromatic
375 moieties that are present also in IBU and IND molecules (Hirano et al. 2013, Jensen et al. 2014).
376 These interactions combined might explain the high T_gs observed also with the 1:2 co-amorphous
377 mixtures.

3.4 Stability studies

To investigate the solid-state stability of the co-amorphous mixtures, as well as comparing them to the stability of the pure amorphous drugs, the materials were stored under three different conditions, namely 4 °C, 0% RH; 25 °C, 60% RH; and 40 °C, 0% RH. However, at 25 °C, 60% RH condition, both of the spray dried IBU-ARG mixtures and the spray dried IND-ARG 1:2 mixture transformed into sticky liquids already before the first XRPD and FTIR measurements at day 7. This liquefaction was due to the moisture absorbed by the hygroscopic amorphous material. With other material-condition combinations, the stability study was continued for one year, or until the first signs of crystallization were observed in the X-ray diffractograms. The X-ray diffractograms and the FTIR spectra at the end of the study are presented in Figure 4.

The diffractogram of cryomilled IND showed peaks of crystalline IND already after 7 days of storage regardless of the storage condition, which is in accordance with previous findings (Löbmann et al. 2013a). The features of crystalline IND could be observed also from the FTIR spectra of the stored samples.

The recrystallization of both IBU and IND seemed to be effectively prevented by combining them with ARG as a co-amorphous mixture. No diffraction peaks were identified in the diffractograms of the different mixtures during an approximately 1 year period regardless of the storage condition. Additionally, the FTIR spectra remained unchanged when compared to the spectra recorded at day 0. However, the appearance of many of the powders changed from a fine powder to a more sugar-like form with larger particle size, and with some material-condition combinations, i.e. IND-ARG 1:1 in 25 °C, 60% RH and IBU-ARG 1:2 in 40 °C, 0% RH, the measurements could be performed only until weeks 9 and 14, respectively, due to the increased stickiness of the powders. This change in appearance was similar to that observed with some materials during the first week of the stability study, and was attributed to the absorption of moisture either during the storage (25 °C, 60% RH) or the measurements (40 °C, 0% RH).

403 The increased physical stability of co-amorphous IND-ARG 1:1 mixtures has been established
404 previously, and it has been attributed to the strong interactions between the components and the
405 consequent increased T_g, as well as to the molecular level mixing and the amino acids acting as
406 impurities in the structure of the amorphous drug. With the co-amorphous IBU-ARG 1:1 mixture, the
407 high physical stability together with the high T_g and the features in FTIR spectrum further evidence
408 of the strong interactions (salt formation) between IBU and ARG as well. The salt formation has been
409 previously shown to stabilize amorphous IBU also in the mixture of IBU and kaolin, but with kaolin,
410 IBU could not be completely transformed into an amorphous form (Mallick et al. 2008). A complete
411 amorphization and subsequent high physical stability of IBU has been observed at least with
412 mesoporous carrier materials (silica and magnesium carbonite (Upsalite®)) (Shen et al. 2010; Zhang
413 et al. 2014). When compared to these methods, however, the use of ARG as a co-former is simple,
414 since no processing of the starting materials is required prior to the spray drying.

415 Previously, several studies have suggested that the co-amorphous mixtures of molar ratio of 1:1 would
416 possess the optimal physical stability when the components interact with each other e.g. by forming
417 a salt or heterodimer (Allesø et al. 2009; Chieng et al. 2009; Löbmann et al. 2011). With other molar
418 ratios, it has often been observed that the excess component will recrystallize first and relatively fast,
419 unless mechanisms other than strong molecular interactions stabilize the mixture (Löbmann et al.
420 2012). In the present study, however, no crystallization was observed with either the 1:1 or the 1:2
421 mixture by the date of the submission. Similar behavior has been recently observed also with other
422 co-amorphous mixtures. The mixtures of tranilast and diphenhydramine at different molar ratios (2:1,
423 1:1 and 1:2) remained amorphous throughout the 30-day stability test (Ueda et al. 2017). The
424 improved stability of these mixtures when compared to amorphous single components was attributed
425 to intermolecular interactions (hydrogen bonds and π-π stacking), but the differences in the stabilizing
426 factors between mixtures of different molar ratios remained unassessed. Instead, with co-amorphous
427 naproxen-IND mixtures, the molar ratio of 60:40 was found to be the eutectic composition, and thus

428 the most stable (Beyer et al. 2016a). Due to this observation, the physical drug-ARG mixtures of
429 different mass ratios were investigated with DSC to observe the possible formation of eutectic
430 mixture. However, the thermal events of physical mixtures were rather consistent with those of the
431 single components, and no eutectic melting was observed (Figures S5 and S6). The FTIR spectra of
432 the co-amorphous IBU-ARG and IND-ARG mixtures of the present study suggested the possibility
433 of hydrogen bonding in addition to the salt formation, which might also explain the high stability of
434 the 1:2 mixtures. Additionally, the previously observed interactions between ARG and aromatic
435 structures may stabilize both 1:1 and 1:2 mixtures (Jensen et al 2014, Hirano et al. 2013).

436 **3.5 Dissolution studies**

437 We conducted 24h powder dissolution studies in order to compare the dissolution properties of the
438 spray dried drug-ARG mixtures to the dissolution properties of the mixtures of crystalline drug and
439 crystalline ARG (physical mixtures) and the plain crystalline drug. The results of the dissolution
440 studies with different IBU-ARG and IND-ARG combinations are presented in Figure 5. However,
441 the dissolution profiles obtained in the phosphate buffer (pH 7.2) are shown only in the supplementary
442 material (Figure S7), since at that pH, the effect of co-amorphization or the presence of ARG seemed
443 to have been overruled by the effect of high pH on the dissolution of acidic drugs.

444 At a pH of 1.2, the cumulative dissolved amount of IBU (approximately 50% at 24h) from pure
445 crystalline powder remained lower when compared to the other formulations throughout the whole
446 experiment, and the difference was also statistically significant between the majority of the samples.
447 The impact of ARG on the dissolution of IBU was obvious, since the physical mixtures reached the
448 50% cumulative dissolved amount already before 2h (1:1 mixture) or 1h (1:2 mixture) time points,
449 and the total cumulative dissolved amount ranged from 74% (1:1 mixture) to 83% (1:2 mixture).
450 However, according to the statistical analysis, no significant difference was observed between the
451 two physical mixtures. In addition to the presence of ARG, the formation of a co-amorphous mixture
452 seemed to enhance the dissolution of IBU. When compared to the corresponding physical mixture,

453 the cumulative dissolved amounts were statistically significantly higher at 30 min and 60 min time
454 points (1:1 mixture), and until 2h time point (1:2 mixture).

455 With IND at a pH of 1.2, the detection limit was only exceeded with spray dried IND-ARG mixtures
456 of which the 1:2 mixture produced detectable concentrations from 1h onwards, whereas with 1:1
457 mixture this happened only at 4h. Thus, the dissolution studies with IND and IND-ARG mixtures
458 were conducted also in acetate buffer of pH of 5.0 to obtain measurable concentrations also from the
459 less soluble formulations. At pH of 5.0, the dissolution profile of the plain γIND resembled the
460 profiles of the physical mixtures. However, the spray dried co-amorphous mixtures seemed to
461 dissolve much more rapidly and more completely when compared to the other formulations. This was
462 confirmed by the statistical analysis that suggested significantly higher cumulative dissolved amounts
463 of IND from 30 min onwards with 1:1 co-amorphous mixture and at every time point with 1:2 co-
464 amorphous mixture when compared to γIND or the physical mixtures. Additionally, the co-
465 amorphous 1:2 IND-ARG mixture produced significantly higher cumulative dissolved amounts of
466 IND at almost every time point when compared to the co-amorphous 1:1 mixture.

467 The increase in intrinsic dissolution rate with either ball milled or spray dried co-amorphous IND-
468 ARG 1:1 mixtures when compared to crystalline or amorphous IND has been observed previously by
469 Löbmann et al. and Jensen et al. (Jensen et al. 2016a; Löbmann et al. 2013a). However, in these
470 studies, the intrinsic dissolution tests have only been conducted at pH of 7.2, whereas our findings
471 suggest that even more pronounced differences might have occurred at lower pH values. Additionally,
472 to the best of our knowledge, this is the first time that the dissolution properties of the IND-ARG 1:2
473 mixture have been studied. Somewhat surprisingly, the dissolution was even more rapid and more
474 complete with the molar ratio of 1:2 than with molar ratio of 1:1, which suggests that 1:1 salt
475 formation is not the only solubilizing interaction between IND and ARG. This suggestion is in
476 accordance with predictions based on our FTIR measurements.

As far as we are aware, the co-amorphous mixtures of IBU and ARG have not been prepared or investigated previously. However, Fini et al. (1985) have studied the solubility of equimolar IBU-ARG salt, and found the higher dissolution rate when compared to the acid form of IBU especially at low pH values. This could be predicted also based on the present study, since also the physical mixtures increased the dissolution rate when compared to the pure crystalline IBU. Furthermore, the difference between the dissolution profiles of the co-amorphous mixtures and the physical mixtures was not as significant as with the IND-ARG mixtures, which might suggest that the salt formation dominates the possible other solubilizing interactions between IBU and ARG during dissolution. However, also with IBU-ARG, the co-amorphous mixture of molar ratio of 1:2 dissolved more rapidly and more completely when compared to 1:1 mixture, which underlines the need for further studies on the drug-ARG interactions in solution.

The strong influence of pH on the dissolution of both IBU and IND may be attributed to their pK_a values that lie between 4.5 and 5 (ElShaer et al. 2011; Tilborg et al. 2014). Thus, it was expected that at a pH of 1.2, the drugs remain unionized and poorly soluble, whereas at pH of 7.2, their dissolution is enhanced due to almost complete ionization. Additionally, the pH dependence of the effect of ARG on the dissolution of the drugs may be attributed to the differences in the ionization of the drugs between the media of different pH. At higher pH values, the drugs were almost completely ionized regardless of the presence of ARG, whereas at lower pH, the interactions (salt formation) between acidic drug and basic ARG became significant.

The transit time through stomach and small intestine (main site for absorption) has been estimated to be only less than 5h (Abuhelwa et al. 2016a; Yuen 2010). Thus, to ensure adequate absorption and bioavailability, the drugs should dissolve already in the early parts of the small intestine. This rapid dissolution may be challenging for acidic drugs, since the pH of the intestinal fluids is generally lowest at the beginning of the gastrointestinal tract (Abuhelwa et al. 2016b). However, the elevated dissolution rate and cumulative dissolved amount of IBU and IND from co-amorphous drug-ARG

mixtures in low pH conditions suggests that the formation of co-amorphous salt may be a potential method in increasing the bioavailability of acidic drugs even though further studies are required.

4. CONCLUSIONS

The aim of the present study was to produce stable co-amorphous IBU-ARG and IND-ARG mixtures with enhanced dissolution properties by spray drying from pure aqueous solutions. According to solid state studies, the spray dried IBU-ARG and IND-ARG mixtures of molar ratios of 1:1 and 1:2 were X-ray amorphous and possessed single T_g. Additionally, FTIR analysis revealed strong interactions (e.g. salt formation) between both drugs and ARG. The physical stability of the co-amorphous mixtures was significantly improved when compared to the pure amorphous drugs, although the absorbance of moisture may cause handling difficulties especially with IBU-ARG mixtures. Furthermore, at low pH, the co-amorphous mixtures dissolved more rapidly and more completely when compared to the physical mixtures of the drug and ARG or to the pure drugs. This dissolution enhancement might increase the amount of dissolved drug at the beginning of the gastrointestinal tract, which again might improve bioavailability. In conclusion, spray drying seems to be a potential up-scalable method for preparing co-amorphous mixtures that possess improved physical stability and dissolution characteristics. Additionally, the use of organic solvents and surfactants may be avoided if the appropriate co-former solubilizes the drug adequately.

ACKNOWLEDGEMENT

RO acknowledges the support from the Doctoral Programme in Drug Research in the Doctoral School of University of Eastern Finland.

APPENDIX A. Supplementary material

Supplementary material associated with this article can be found in the online version

REFERENCES

525 Abuhelwa, A.Y., Foster, D.J.R., Upton, R.N., 2016a. A Quantitative Review and Meta-models of
526 the Variability and Factors Affecting Oral Drug Absorption—Part II: Gastrointestinal Transit Time.
527 AAPS J., 18, 1322-1333. https://doi.org/10.1208/s12248-016-9953-7.

528 Abuhelwa, A.Y., Foster, D.J.R., Upton, R.N., 2016b. A Quantitative Review and Meta-Models of
529 the Variability and Factors Affecting Oral Drug Absorption—Part I: Gastrointestinal pH. AAPS J.,
530 18, 1309-1321. https://doi.org/10.1208/s12248-016-9952-8.

531 Agrawal, A.M., Dudhedia, M.S., Patel, A.D., Raikes, M.S., 2013. Characterization and performance
532 assessment of solid dispersions prepared by hot melt extrusion and spray drying process. Int. J.
533 Pharm., 457, 71-81. https://doi.org/10.1016/j.ijpharm.2013.08.081.

534 Allesø, M., Chieng, N., Rehder, S., Rantanen, J., Rades, T., Aaltonen, J., 2009. Enhanced
535 dissolution rate and synchronized release of drugs in binary systems through formulation:
536 Amorphous naproxen-cimetidine mixtures prepared by mechanical activation. J. Control. Release,
537 136, 45-53. https://doi.org/10.1016/j.jconrel.2009.01.027.

538 Baghel, S., Cathcart, H., O'Reilly, N.J., 2016. Polymeric Amorphous Solid Dispersions: A Review
539 of Amorphization, Crystallization, Stabilization, Solid-State Characterization, and Aqueous
540 Solubilization of Biopharmaceutical Classification System Class II Drugs. J. Pharm. Sci., 105,
541 2527-2544. https://doi.org/10.1016/j.xphs.2015.10.008.

542 Baird, J.A., Taylor, L.S., 2012. Evaluation of amorphous solid dispersion properties using thermal
543 analysis techniques. Adv. Drug Deliv. Rev., 64, 396-421.
544 https://doi.org/10.1016/j.addr.2011.07.009.

545 Beyer, A., Grohganz, H., Löbmann, K., Rades, T., Leopold, C.S., 2016a. Influence of the cooling
546 rate and the blend ratio on the physical stability of co-amorphous naproxen/indomethacin. Eur. J.
547 Pharm. Biopharm., 109, 140-148. https://doi.org/10.1016/j.ejpb.2016.10.002.

548 Beyer, A., Radi, L., Grohganz, H., Löbmann, K., Rades, T., Leopold, C.S., 2016b. Preparation and
549 recrystallization behavior of spray-dried co-amorphous naproxen-indomethacin. Eur. J. Pharm.
550 Biopharm., 104, 72-81. https://doi.org/10.1016/j.ejpb.2016.04.019.

551 Bruzzese, T., Ferrari, R., 1981. Method of relieving pain and treating inflammatory conditions in
552 warm-blooded animals. A61K 31/205 424/316 US 4,279,926, 3.8.1979.

553 Chavan, R.B., Thipparaboina, R., Kumar, D., Shastri, N.R., 2016. Co amorphous systems: A
554 product development perspective. Int. J. Pharm., 515, 403-415.
555 https://doi.org/10.1016/j.ijpharm.2016.10.043.

556 Chieng, N., Aaltonen, J., Saville, D., Rades, T., 2009. Physical characterization and stability of
557 amorphous indomethacin and ranitidine hydrochloride binary systems prepared by mechanical
558 activation. Eur. J. Pharm. Biopharm., 71, 47-54. https://doi.org/10.1016/j.ejpb.2008.06.022.

559 Craye, G., Löbmann, K., Grohganz, H., Rades, T., Laitinen, R., McPhee, D.J., 2015.
560 Characterization of amorphous and co-amorphous simvastatin formulations prepared by spray
561 drying. Molecules, 20, 21532-21548. https://doi.org/10.3390/molecules201219784.

562 Cristofoletti, R., Dressman, J.B., 2017. Dissolution Methods to Increasing Discriminatory Power of
563 In Vitro Dissolution Testing for Ibuprofen Free Acid and Its Salts. J. Pharm. Sci., 106, 92-99.
564 https://doi.org/10.1016/j.xphs.2016.06.001.

565 De Brabander, C., Van Den Mooter, G., Vervaet, C., Remon, J.P., 2002. Characterization of
566 ibuprofen as a nontraditional plasticizer of ethyl cellulose. J. Pharm. Sci., 91, 1678-1685.
567 https://doi.org/10.1002/jps.10159.

568 Dengale, S.J., Grohganz, H., Rades, T., Löbmann, K., 2016. Recent advances in co-amorphous drug
569 formulations. Adv. Drug Deliv. Rev., 100, 116-125. https://doi.org/10.1016/j.addr.2015.12.009.

570 ElShaer, A., Khan, S., Perumal, D., Hanson, P., Mohammed, A.R., 2011. Use of amino acids as
571 counterions improves the solubility of the BCS II model drug, indomethacin. Curr. Drug Deliv., 8,
572 363-372. https://doi.org/10.2174/156720111795767924.

573 Fini, A., Zecchi, V., Tartarini, A., 1985. Dissolution profiles of NSAID carboxylic acids and their
574 salts with different counter ions. Pharm. Acta Helv., 60, 58-62.

575 He, Y., Ho, C., 2015. Amorphous Solid Dispersions: Utilization and Challenges in Drug Discovery
576 and Development. J. Pharm. Sci., 104, 3237-3258. https://doi.org/10.1002/jps.24541.

577 Hirano, A., Kameda, T., Shinozaki, D., Arakawa, T., Shiraki, K., 2013. Molecular dynamics
578 simulation of the arginine-assisted solubilization of caffeic acid: intervention in the interaction. J
579 Phys Chem B, 117, 7518-7527. https://doi.org/10.1021/jp401609p.

580 Izutsu, K.-., Fujimaki, Y., Kuwabara, A., Aoyagi, N., 2005. Effect of counterions on the physical
581 properties of L-arginine in frozen solutions and freeze-dried solids. Int. J. Pharm., 301, 161-169.
582 https://doi.org/10.1016/j.ijpharm.2005.05.019.

583 Jensen, K.T., Blaabjerg, L.I., Lenz, E., Bohr, A., Grohganz, H., Kleinebudde, P., Rades, T.,
584 Löbmann, K., 2016a. Preparation and characterization of spray-dried co-amorphous drug-amino
585 acid salts. J. Pharm. Pharmacol., 68, 615-624. https://doi.org/10.1111/jphp.12458.

586 Jensen, K.T., Larsen, F.H., Löbmann, K., Rades, T., Grohganz, H., 2016b. Influence of variation in
587 molar ratio on co-amorphous drug-amino acid systems. Eur. J. Pharm. Biopharm., 107, 32-39.
588 https://doi.org/10.1016/j.ejpb.2016.06.020.

589 Jensen, K.T., Löbmann, K., Rades, T., Grohganz, H., 2014. Improving co-amorphous drug
590 formulations by the addition of the highly water soluble amino Acid, proline. Pharmaceutics, 6,
591 416-435. https://doi.org/10.3390/pharmaceutics6030416.

592 Kyerematen, S.O., Pudlas, M., Woehrle, G.H., 2014. A fast and reliable empirical approach for
593 estimating solubility of crystalline drugs in polymers for hot melt extrusion formulations. J. Pharm.
594 Sci., 103, 2847-2858. https://doi.org/10.1002/jps.23941.

595 Laitinen, R., Löbmann, K., Strachan, C.J., Grohganz, H., Rades, T., 2013. Emerging trends in the
596 stabilization of amorphous drugs. Int. J. Pharm., 453, 65-79.
597 https://doi.org/10.1016/j.ijpharm.2012.04.066.

598 Lakio, S., Morton, D.A.V., Ralph, A.P., Lambert, P., 2015. Optimizing aerosolization of a high-
599 dose L-arginine powder for pulmonary delivery. Asian J. Pharm. Sci. 10, 528-540.
600 http://dx.doi.org/10.1016/j.ajps.2015.08.001

601 Lee, T., Wang, Y.W., 2009. Initial salt screening procedures for manufacturing ibuprofen. Drug
602 Dev. Ind. Pharm., 35, 555-567. https://doi.org/10.1080/03639040802459452.

603 Lipinski, C.A., Lombardo, F., Dominy, B.W., Feeney, P.J., 2001. Experimental and computational
604 approaches to estimate solubility and permeability in drug discovery and development settings.
605 Adv. Drug Deliv. Rev., 46, 3-26. https://doi.org/10.1016/S0169-409X(00)00129-0.

606 Lipiäinen, T., Peltoniemi, M., Räikkönen, H., Juppo, A., 2016. Spray-dried amorphous isomalt and
607 melibiose, two potential protein-stabilizing excipients. Int. J. Pharm., 510, 311-322.
608 http://dx.doi.org/10.1016/j.ijpharm.2016.06.038

609 Löbmann, K., Grohganz, H., Laitinen, R., Strachan, C., Rades, T., 2013a. Amino acids as co-
610 amorphous stabilizers for poorly water soluble drugs--Part 1: preparation, stability and dissolution
611 enhancement. Eur. J. Pharm. Biopharm., 85, 873-881. https://doi.org/10.1016/j.ejpb.2013.03.014.

612 Löbmann, K., Laitinen, R., Grohganz, H., Gordon, K.C., Strachan, C., Rades, T., 2011.
613 Coamorphous drug systems: enhanced physical stability and dissolution rate of indomethacin and
614 naproxen. Mol. Pharm., 8, 1919-1928. https://doi.org/10.1021/mp2002973.

615 Löbmann, K., Laitinen, R., Grohganz, H., Strachan, C., Rades, T., Gordon, K.C., 2013b. A
616 theoretical and spectroscopic study of co-amorphous naproxen and indomethacin. Int. J. Pharm.,
617 453, 80-87. https://doi.org/10.1016/j.ijpharm.2012.05.016.

618 Löbmann, K., Laitinen, R., Strachan, C., Rades, T., Grohganz, H., 2013c. Amino acids as co-
619 amorphous stabilizers for poorly water-soluble drugs--Part 2: molecular interactions. Eur. J. Pharm.
620 Biopharm., 85, 882-888. https://doi.org/10.1016/j.ejpb.2013.03.026.

621 Löbmann, K., Strachan, C., Grohganz, H., Rades, T., Korhonen, O., Laitinen, R., 2012. Co-
622 amorphous simvastatin and glipizide combinations show improved physical stability without
623 evidence of intermolecular interactions. Eur. J. Pharm. Biopharm., 81, 159-169.
624 https://doi.org/10.1016/j.ejpb.2012.02.004.

625 Mallick, S., Pattnaik, S., Swain, K., De, P.K., Saha, A., Ghoshal, G., Mondal, A., 2008. Formation
626 of physically stable amorphous phase of ibuprofen by solid state milling with kaolin. Eur. J. Pharm.
627 Biopharm., 68, 346-351. https://doi.org/10.1016/j.ejpb.2007.06.003.

628 Meng, F., Gala, U., Chauhan, H., 2015. Classification of solid dispersions: Correlation to (i)
629 stability and solubility (II) preparation and characterization techniques. Drug Dev. Ind. Pharm., 41,
630 1401-1415. https://doi.org/10.3109/03639045.2015.1018274.

631 Ojarinta, R., Heikkinen, A.T., Sievänen, E., Laitinen, R., 2017. Dissolution behavior of co-
632 amorphous amino acid-indomethacin mixtures: The ability of amino acids to stabilize the
633 supersaturated state of indomethacin. Eur. J. Pharm. Biopharm., 112, 85-95.
634 https://doi.org/10.1016/j.ejpb.2016.11.023.

635 Sakurai, A., Sako, K., Maitani, Y., 2012. Influence of manufacturing factors on physical stability
636 and solubility of solid dispersions containing a low glass transition temperature drug. Chem. Pharm.
637 Bull., 60, 1366-1371. https://doi.org/10.1248/cpb.c12-00354.

638 Shen, S.-., Ng, W.K., Chia, L., Dong, Y.-., Tan, R.B.H., 2010. Stabilized amorphous state of
639 ibuprofen by co-spray drying with mesoporous SBA-15 to enhance dissolution properties. J. Pharm.
640 Sci., 99, 1997-2007. https://doi.org/10.1002/jps.21967.

641 Stroppolo, F., Bonadeo, D., Gazzaniga, A., 1995. Process for the preparation of salts of 2-(4-
642 isobutylphenyl)propionic acid. C07C 53/134 562/496 US 5,463,117, 29.7.1994.

643 Tilborg, A., Norberg, B., Wouters, J., 2014. Pharmaceutical salts and cocrystals involving amino
644 acids: A brief structural overview of the state-of-art. Eur. J. Med. Chem., 74, 411-426.
645 https://doi.org/10.1016/j.ejmech.2013.11.045.

646 Tong, P., Zografi, G., 1999. Solid-state characteristics of amorphous sodium indomethacin relative
647 to its free acid. Pharm. Res., 16, 1186-1192. https://doi.org/10.1023/A:1018985110956.

648 Ueda, H., Kadota, K., Imono, M., Ito, T., Kunita, A., Tozuka, Y., 2017. Co-amorphous Formation
649 Induced by Combination of Tranilast and Diphenhydramine Hydrochloride. J. Pharm. Sci., 106,
650 123-128. https://doi.org/10.1016/j.xphs.2016.07.009.

651 Van Den Mooter, G., 2012. The use of amorphous solid dispersions: A formulation strategy to
652 overcome poor solubility and dissolution rate. Drug Discov. Today Techn., 9, e79-e85.
653 https://doi.org/10.1016/j.ddtec.2011.10.002.

654 Vasconcelos, T., Marques, S., das Neves, J., Sarmento, B., 2016. Amorphous solid dispersions:
655 Rational selection of a manufacturing process. Adv. Drug Deliv. Rev., 100, 85-101.
656 https://doi.org/10.1016/j.addr.2016.01.012.

657 Vo, C.L., Park, C., Lee, B.-., 2013. Current trends and future perspectives of solid dispersions
658 containing poorly water-soluble drugs. Eur. J. Pharm. Biopharm., 85, 799-813.
659 https://doi.org/10.1016/j.ejpb.2013.09.007.

660 Wiranidchapong, C., Ruangpayungsak, N., Suwattanasuk, P., Shuwisitkul, D., Tanvichien, S., 2015.
661 Plasticizing effect of ibuprofen induced an alteration of drug released from Kollidon SR matrices
662 produced by direct compression. Drug Dev. Ind. Pharm., 41, 1037-1046.
663 https://doi.org/10.3109/03639045.2014.925917.

664 Yuen, K., 2010. The transit of dosage forms through the small intestine. Int. J. Pharm., 395, 9-16.
665 https://doi.org/10.1016/j.ijpharm.2010.04.045.

666 Zhang, F., Aaltonen, J., Tian, F., Saville, D.J., Rades, T., 2009. Influence of particle size and
667 preparation methods on the physical and chemical stability of amorphous simvastatin. Eur. J.
668 Pharm. Biopharm., 71, 64-70. https://doi.org/10.1016/j.ejpb.2008.07.010.

669 Zhang, P., Forsgren, J., Strømme, M., 2014. Stabilisation of amorphous ibuprofen in Upsalite, a
670 mesoporous magnesium carbonate, as an approach to increasing the aqueous solubility of poorly
671 soluble drugs. Int. J. Pharm., 472, 185-191. https://doi.org/10.1016/j.ijpharm.2014.06.025.

TABLES

Table 1. The equilibrium solubilities of ibuprofen (IBU) and indomethacin (IND) in arginine (ARG) solutions of different concentrations (ambient conditions).

ARG (% m/V)	IBU (mg/ml)	IND (mg/ml)
1	2.2 ± 0.45	5.2 ± 2.0
5	47.0 ± 3.8	98.1 ± 4.1
10	56.9 ± 22.4	174.5 ± 27.1

Table 2. The glass transition temperatures (mid-point; T_g exp.) of the spray dried arginine (ARG), quench cooled ibuprofen (IBU), cryomilled indomethacin (IND), and the spray dried IBU-ARG and IND-ARG mixtures of different molar ratios. When applicable, also literature values of T_gs (T_g lit.) and predicted T_gs ($T_{g,\,mix}$) based on Gordon-Taylor equation are shown.

	T_g (°C) exp.	T_g (°C) lit.	$T_{g,\,mix}$ (°C)
ARG[a]	34.0[b]	18.4 (Jensen et al. 2014); 55 (Izutsu et al. 2005)	-
IBU[c]	-42.8 ± 0.01	-43.6 (De Brabander et al. 2002); -44.1 (Wiranidchapong et al. 2015)	-
IND[d]	43.97 ± 0.26	36.7 (Löbmann et al. 2013a); 44.7 (Tong and Zografi 1999)	-
IBU-ARG 1:1[a]	82.8 ± 1.93	-	-10.2
IBU-ARG 1:2[a]	83.1 ± 0.29	-	6.1
IND-ARG 1:1[a]	111.7 ± 0.12	64.1[e] (Löbmann et al. 2013a);114.1[a] (Jensen et al. 2016a)	48.7
IND-ARG 1:2[a]	102.9 ± 1.92	-	50.3

[a] Spray dried [c] In situ quench cooled [e] Ball milled
[b] Only one observation [d] Cryomilled

LIST OF FIGURES

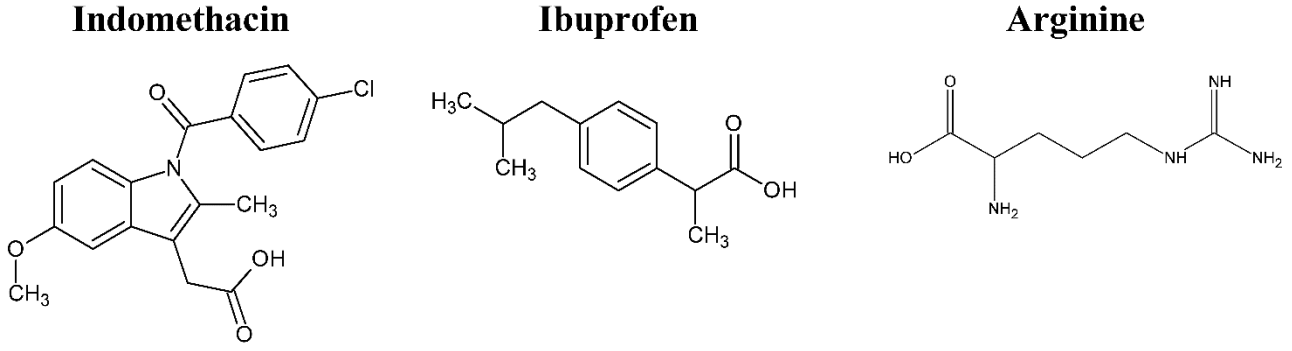

Figure 1. The Chemical structures of arginine, ibuprofen and indomethacin.

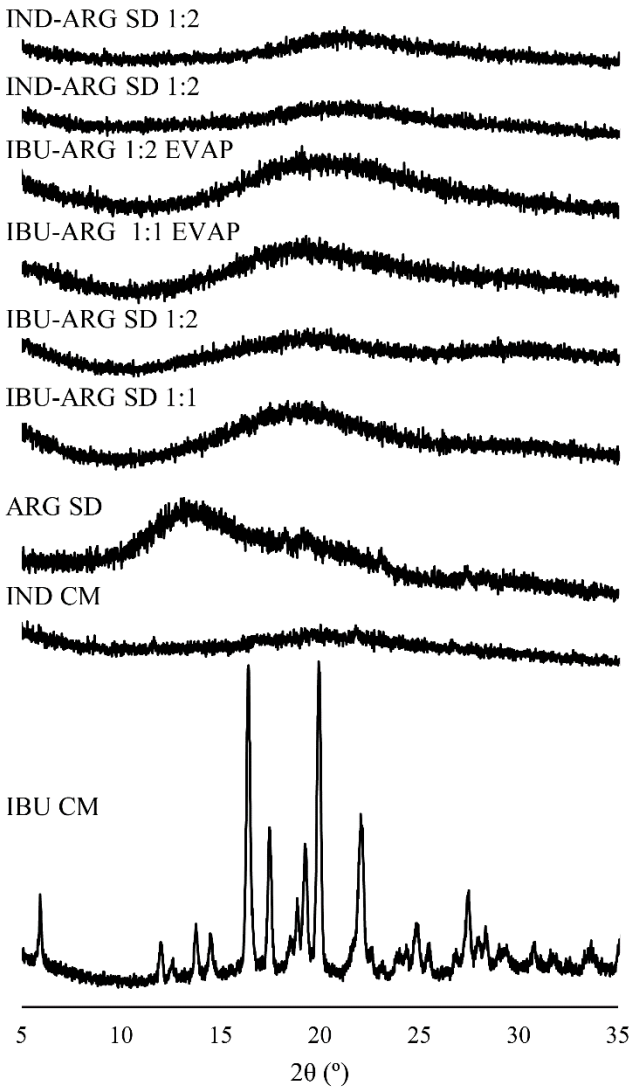

684

685 **Figure 2.** Diffractograms of cryomilled (CM) ibuprofen (IBU), CM indomethacin (IND), spray
686 dried (SD) arginine (ARG), SD IBU-ARG and IND-ARG mixtures of different molar ratios, and
687 IBU-ARG mixtures prepared by slowly evaporating the water (EVAP).

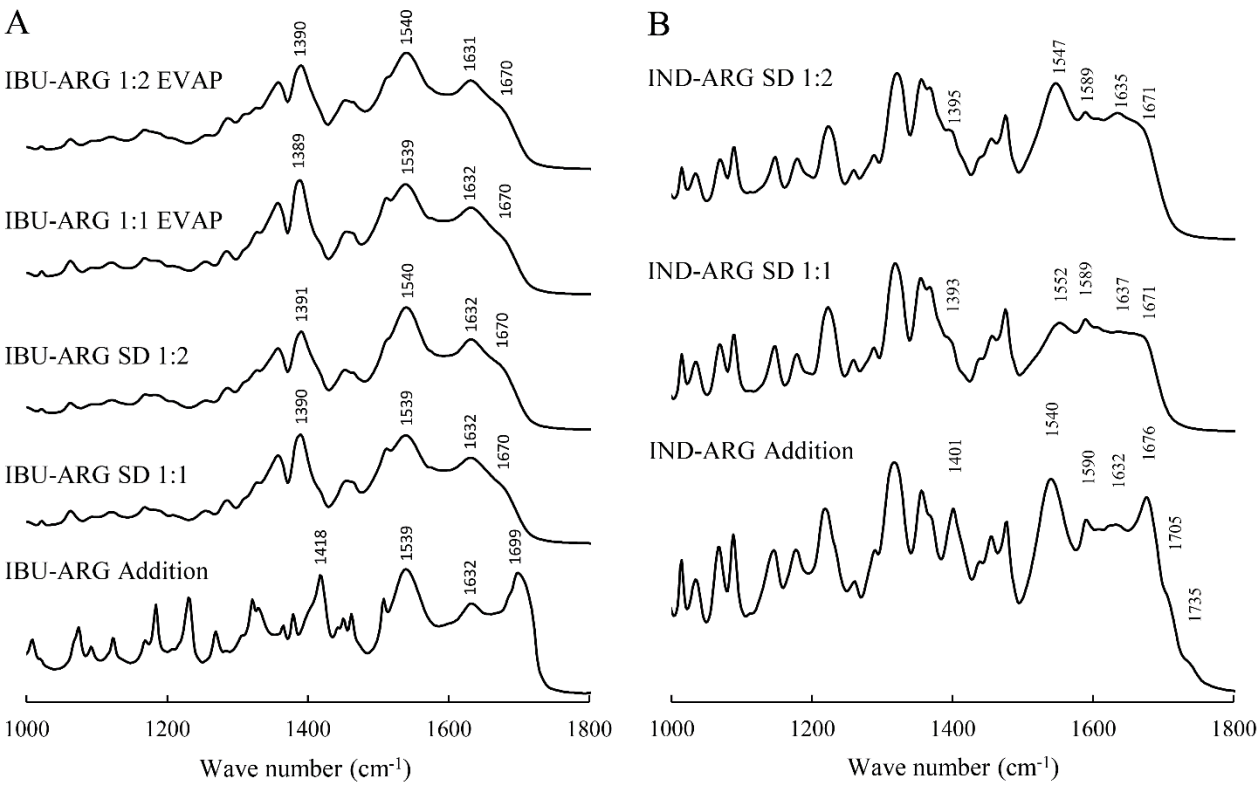

688

689 **Figure 3.** The measured FTIR spectra of ibuprofen-arginine (A; IBU-ARG) and indomethacin-
690 arginine (B; IND-ARG) mixtures of different molar ratios prepared by spray drying (SD) or by
691 slowly evaporating the solvent water (EVAP). The calculated addition spectra of crystalline IBU
692 and amorphous ARG as well as amorphous IND and amorphous ARG are also included.

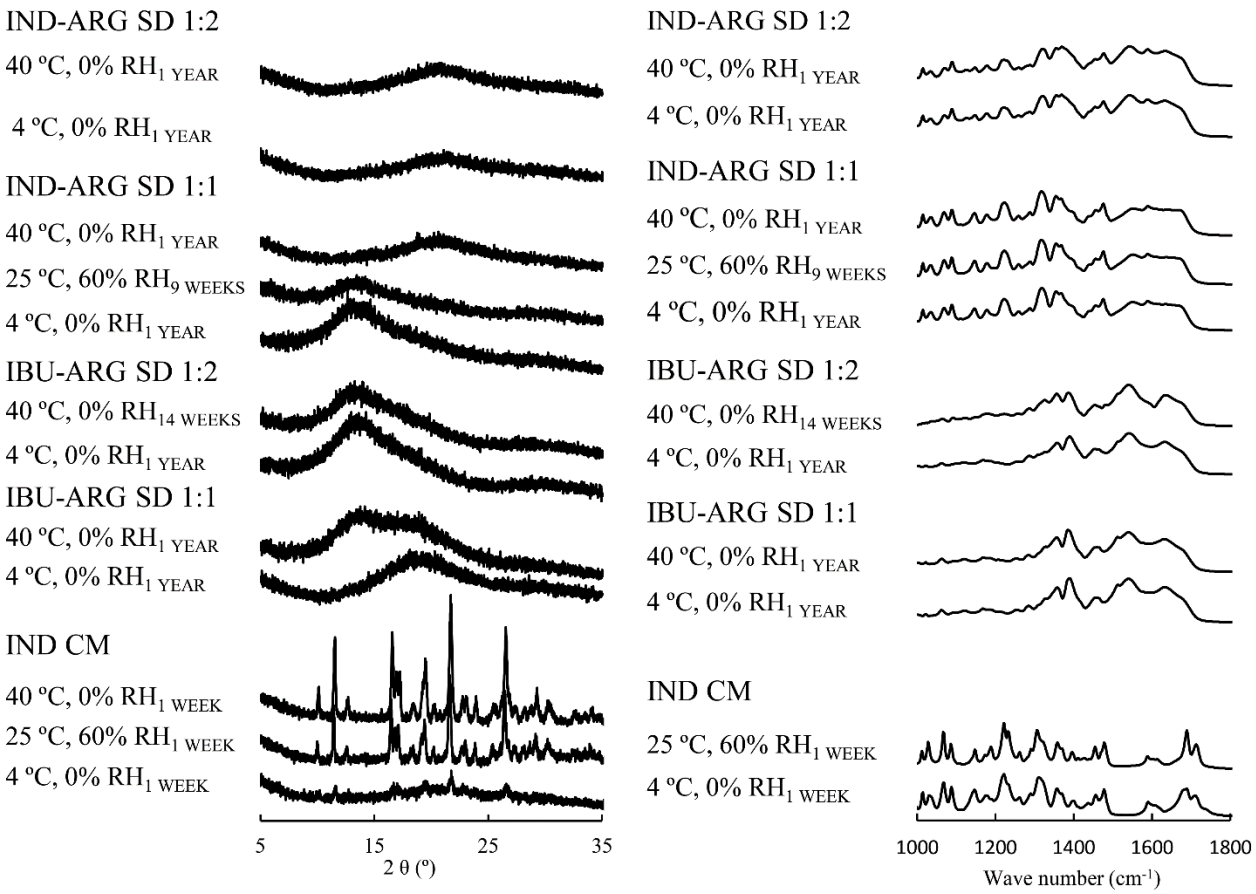

693

694 **Figure 4.** The X-ray diffractograms and FTIR spectra of spray dried (SD) ibuprofen-arginine (IBU-
695 ARG) and indomethacin-arginine (IND-ARG) mixtures after storing them under different
696 conditions for different periods of time. The diffractograms and FTIR spectra of cryomilled (CM)
697 IND are also included for comparison.

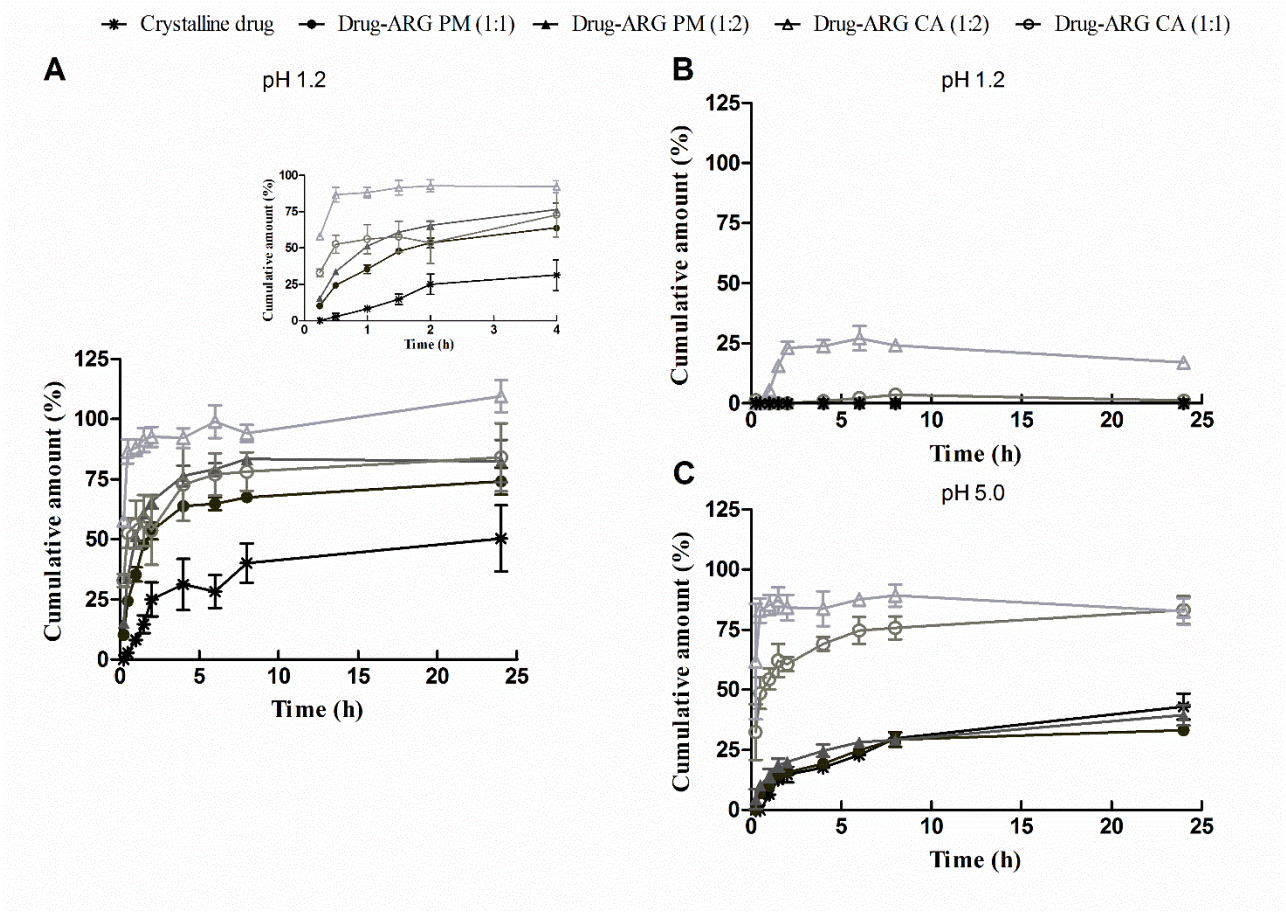

698

699 **Figure 5.** The cumulative dissolved amount of ibuprofen (A, pH 1.2) and indomethacin (B, pH 1.2;
700 C, pH 5.0) from crystalline drug, from physical mixtures (PM) of drug and arginine (ARG) (1:1 and
701 1.2), and from spray dried (SD) drug-ARG mixtures (1:1 and 1:2). The first four hours of the
702 dissolution test with IBU have been enlarged.

703